

Probing (Ultra-) Light Dark Matter Using Synchrotron Based Mössbauer Spectroscopy

Abhishek Banerjee ^{1,*}

¹*Maryland Center for Fundamental Physics, University of Maryland, College Park, MD 20742, USA*

(Dated: August 12, 2024)

We propose to search for (ultra)-light scalar dark matter (DM) using synchrotron radiation based Mössbauer spectroscopy technique. Such DM induces temporal variation in various fundamental constants, which in turn causes time modulation of the nuclear transition energies. When a Mössbauer source and absorber is separated by a large baseline, the DM induced shift between their energy levels can be tested by the modulation of the photon absorption spectrum. The narrow Mössbauer transitions allow the setup to efficiently probe DM in the high frequency range. We show that the reach of a Mössbauer experiment with the existing synchrotron beams is at par with the bounds from various equivalence principle violation searches. An improvement of the synchrotron setup would enable us to probe the hitherto uncharted territory of the DM parameter space upto MHz frequency. The proposed method would extend the DM search beyond the EP limit by several orders of magnitude, and would provide the best bound on DM interaction strength with various standard model fields in the high (>kHz) frequency region.

I. INTRODUCTION

Unveiling the nature of dark matter (DM), which accounts for 25% of the energy budget of the universe, is one of the main quests of modern physics. Ultra-light (sub-eV) bosonic fields are natural dark matter candidates [1]. They emerge in a number of theories aimed at solving outstanding problems of particle physics such as the strong CP [2–10] and hierarchy problems [11–15]. If such particles exist, due to the misalignment mechanism, they are generically expected to have a cosmic abundance which can easily be all of the dark matter [16–18]. These strong theory motivations have sparked a significant experimental program aimed at discovering a broad range of such interactions [19–22].

The key idea behind these experiments is as follows. The energy density in ultra-light dark matter (ULDM) is contained in coherent oscillations of the classical field $\phi(t, \vec{x})$ associated with the dark matter particle (ϕ). The oscillations occur at a frequency equal to the mass m_ϕ of the dark matter, with a width $\sim 10^{-6}m_\phi$ determined by the kinetic energy of the dark matter in the galaxy. When these particles interact with the standard model (SM), these coherent oscillations lead to time dependent signatures over a narrow frequency band. These narrow band signatures are the prime targets of these experiments.

One of the generic kinds of interactions that these particles can have with the standard model is via CP-even moduli-like interactions where the oscillating dark matter field results in oscillations in various fundamental constants such as the fine structure constant, quark and lepton masses and the QCD scale. These kinds of dark matter interactions can be probed by looking for frequency comparisons between two sources of stable frequencies, typically realized via a suitable atomic clock system [23–26]. In such systems, the time needed to drive the requisite clock (or interferometric) transitions limits the high frequency (> kHz) reach, despite their exquisite sensitivity [27–30]. Moreover, atomic clock systems are sensitive to electronic levels and thus have reduced sensitivity to physics that affects nuclear parameters. Given these challenges, it is interesting to develop techniques that can broaden the search for such physics.

In this work, we propose the use of Mössbauer spectroscopy to probe ultralight dark matter in the kHz-MHz mass range. Mössbauer spectroscopy is an age old technique, based on the recoil free resonant absorption of the emitted photon by a nucleus in a solid [31–33]. Usually the set up consists of a lattice of some specific radio nuclei which emits photons (emitter), and another lattice with the same nuclei in the ground state to absorb (absorber) the emitted photons. The photon absorption spectrum is tested in a spectroscope (see [34–36] and refs. therein). To probe DM, we take a Mössbauer emitter and absorber and separate

* abanerj4@umd.edu

them by a baseline. The dark matter background alters the nuclear transition energy of the emitter and the absorber. When the Mössbauer emitter produces a photon, in the time taken by the photon to traverse the baseline and reach the absorber, the oscillating dark matter field changes the transition energy of the absorber relative to the transition energy of the emitter, leading to modulations in the absorption spectrum of the Mössbauer spectroscopy. The short decay times of the Mössbauer nuclei permits this setup to probe frequencies higher than possible with conventional atomic setups and the system is directly sensitive to physics that changes nuclear properties. To maximize the sensitivity of this setup, it is desirable to have as large a baseline as possible between the emitter and the absorber. In conventional Mössbauer spectroscopy, where the emitter is a suitable radioactive source, the produced photons are not collimated. This limits the achievable baseline. However, with the advent of powerful synchrotron sources, it has now become possible to realize Mössbauer spectroscopy using such sources. In this case, the synchrotron source coherently drives a Mössbauer emitter, resulting in all the nuclei in the sample being driven to the corresponding excited states in phase. The subsequent decay of these nuclei also occurs in phase resulting in an enhanced collimated beam being produced in the forward direction, enabling ~ 100 m - km scale baselines in such setups without loss of flux. For this reason, we will focus our attention on Mössbauer spectroscopy in synchrotron sources.

The rest of this paper is organized as follows. In Section II and Section III, we discuss the setup for the experiment and describe the main theoretical and experimental factors. In Section IV, we discuss the parameters of synchrotron sources that are presently achievable. Using these, in Section V, we estimate the reach for various dark matter - standard model interactions. We describe the results in Section VI and

II. SETUP

Ultra-light bosonic dark matter is described in the galaxy as an oscillating classical field, with the oscillations centered around the mass m_ϕ of the particle with a width $10^{-6}m_\phi$. For concreteness, we will take the example of spin 0 fields, although the described phenomenology can also be extended to vectors [37] and tensors. If this field is the dark matter, its value

in the galaxy is given by:

$$\phi(t, \vec{x}) \simeq \frac{\sqrt{2\rho_{\text{DM}}}}{m_\phi} \cos \left[m_\phi(t + \vec{\beta} \cdot \vec{x}) \right], \quad (2.1)$$

where, the oscillation amplitude is fixed by the requirement that ϕ accounts for 100% of the dark matter (DM) density $\rho_{\text{DM}} \sim 0.4 \text{ GeV}/(\text{cm})^3$, and $|\beta| \sim 10^{-3}$ is the virial velocity. To see how such a dark matter field can give rise to a signal in a Mössbauer spectrometer, assume that the nuclear transition energy E_γ is proportional to ϕ , $E_\gamma = \kappa\phi$ (see section V for specific examples). When this is the case, suppose the emitter (see Figure 1) produces a photon at time t . The energy of the produced photon is $E_\gamma = \kappa\phi(t)$. This photon traverses a baseline of length L when it encounters an absorber. The transition energy at the absorber is $E_\gamma = \kappa\phi(t + L)$. This results in a difference between the emitter and absorber transition energies equal to

$$\Delta E = \kappa \frac{\sqrt{2\rho_{\text{DM}}}}{m_\phi/2} \sin \left(\frac{m_\phi L}{2} \right) \sin \left(m_\phi \left[t + \frac{L}{2} \right] \right). \quad (2.2)$$

The Mössbauer spectrometer can be used to detect this shift with high accuracy. Note that for (2.2) to be valid, the dark matter mass $m_\phi \lesssim \Gamma$ where Γ is the decay width of the Mössbauer transition. This is because the decaying nucleus takes a time $\sim 1/\Gamma$ to produce the photon and modulations at frequencies higher than Γ result in the production of sidebands around the transition energy as opposed to a homogeneous shift to the produced energy. The latter is the case of interest here and it occurs in the limit $m_\phi \lesssim \Gamma$. This signal clearly oscillates at the frequency m_ϕ , the smoking gun signature of ultra-light dark matter (ULDM).

For a qualitative understanding of the signal strength, we can recast Eq. (2.2) as,

$$\Delta E \propto \sqrt{2\rho_{\text{DM}}} L \times \mathcal{W}(m_\phi L/2) \times \sin \left[m_\phi \left(t + \frac{L}{2} \right) \right], \quad (2.3)$$

where, $\mathcal{W}(x) = \text{sinc}(x)$. Notice, $\mathcal{W}(x) \simeq 1$ for very small x , and bounded as $|\mathcal{W}(x)| \lesssim x^{-1}$ for $x \gg 1$. Thus, for a given (non zero) DM mass, the signal is maximized when the baseline $L \sim 1/m_\phi$. Note that, if the total integration time t_{int} is longer than the DM coherence time $\tau_{\text{coh}} = 2\pi/(m_\phi\beta^2)$, the sensitivity of the experiment improves mildly as $t_{\text{int}}^{1/4}$ [38, 39]. Thus, for a given integration time, maximum sensitivity is reached at $m_\phi = 2\pi/(t_{\text{int}}\beta^2)$.

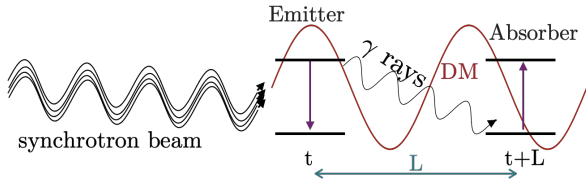


FIG. 1: Proposed set up of the experiment.

III. THEORETICAL AND EXPERIMENTAL CONSIDERATIONS

In this section, we outline the set up for the experiment and describe the main theoretical and experimental factors.

Mössbauer spectroscopy relies on the recoil free resonant absorption of the emitted gamma ray by a nucleus, known as the Mössbauer effect. This is typically observed in the lattice of some specific radio nuclei [31–33]. For a resonance of energy E_0 , and a natural line width Γ , the absorption cross-section σ_{res} , of a photon of energy E_γ can be written as [40],

$$\sigma_{\text{res}}(E_0, E_\gamma, \Gamma) \propto \frac{2\pi}{E_\gamma^2} \frac{(\Gamma/2)^2}{(E_0 - E_\gamma)^2 + (\Gamma/2)^2}, \quad (3.1)$$

for a narrow resonance i.e. $\Gamma/E_0 \ll 1$ [41]. As the Mössbauer transitions are very narrow, an energy shift of $\mathcal{O}(\Gamma)$ by the any perturbation would lead to an “off resonance” transition, and a significant change in the absorption cross section can be observed. This unique property makes it an exciting probe not only for DM but also for new physics discoveries in general [42].

In our case, probing DM involves testing the photon absorption spectrum due to the energy level difference of the Mössbauer source and absorber. Thus, the experimental sensitivity depends on the photon flux at the absorber, which originates from the decay of the Mössbauer source. For a flux of N_γ at the Mössbauer absorber, we obtain the sensitivity of the experiment as

$$\Delta E = \frac{\Gamma}{\sqrt{N_\gamma}}. \quad (3.2)$$

As the source and the absorber are kept close to each other, in conventional Mössbauer spectroscopy, the received flux is equal to the number of observed decays.

One of the challenges of our proposed method is to maintain a high flux of photons even when the Mössbauer emitter and the absorber are far apart. The effective reach of the experiment depends on the number of received photons N_γ , and L , as $\sqrt{N_\gamma} \times L$. Thus a decreasing flux $N_\gamma \propto 1/L^2$ [43], mitigates the apparent gain in sensitivity obtained by a large baseline. At the same time, if the emitted photons are not well collimated (which is the case for a traditional Mössbauer source), the beam diverges quickly; results in an even smaller effective flux at the receiver.

To alleviate the challenges mentioned above, one possibility is to consider synchrotron radiation (SR) based Mössbauer spectroscopy [44–50]. We will denote this set up as synchrotron based Mössbauer spectroscopy or SMS. In SMS, a sample (placed $\sim \mathcal{O}(50\text{m})$ away from the synchrotron source) is directly excited through the absorption of an x-ray photon. In contrast, in conventional Mössbauer spectroscopy, a radioactive parent undergoes decay to generate the desired isotope in the excited state.

In SMS, a synchrotron source coherently excites all the nuclei in the Mössbauer emitter. Thus the subsequent decay of these nuclei also happens in phase in the sense of superradiance [51]. This results in an enhanced collimated beam in the forward direction with a flux equal to the number of resonantly excited Mössbauer source nuclei. However, as the resolution of the synchrotron source, $(\Delta E)_{\text{SR}}$, is much larger than the extremely narrow Mössbauer transitions, only a fraction of the Mössbauer source nuclei would be resonantly excited. Thus, the emitted flux at the Mössbauer source $(N_\gamma)_{\text{MS}}$, can be calculated as,

$$(N_\gamma)_{\text{MS}} = (N_\gamma)_{\text{SR}} \frac{\Gamma}{(\Delta E)_{\text{SR}}}, \quad (3.3)$$

where, $(N_\gamma)_{\text{SR}}$ is the incident synchrotron flux at the Mössbauer source.

To achieve a large statistics, we need to make sure that the flux at the Mössbauer absorber is not significantly reduced. To estimate this, we calculate the Rayleigh range z_R , of a beam. Qualitatively a beam remains parallel over twice the Rayleigh range [40]. To estimate the flux at a distance z , $N_\gamma(z)$, we note that the flux is inversely proportional to the beam area $w^2(z)$, as $N_\gamma(z) \propto 1/w^2(z)$. By expressing $w^2(z)$ in terms of the beam area at the focus w_0^2 ,

and the Rayleigh range, we get

$$N_\gamma(z) \propto \frac{1}{w^2(z)} \propto \frac{1}{w_0^2} \frac{z_R^2}{z^2 + z_R^2}, \quad (3.4)$$

which reproduces the naive scaling of $N_\gamma(z) \propto 1/z^2$ for $z \gg z_R$. The Rayleigh range can be expressed in terms of in terms of focused beam area as

$$z_R = \frac{\pi w_0^2}{\lambda} \sim \frac{\lambda}{\Omega}, \quad (3.5)$$

where, Ω is the angular spread in square radians, and λ is the wavelength. For an extremely collimated SR radiation with $\Omega \sim 10^{-10}$ sr, and $\lambda \sim 10^{-10}$ m, the Rayleigh range is $z_R \sim \mathcal{O}(\text{m})$. Thus, we want to consider a set-up whose Rayleigh range is either large, or comparable to the distance of our interest.

For that purpose, we consider focusing of the emitted photon by using a lens. For a lens with focus length f , and refractive index n , the effective radius of curvature, R_{eff} , can be written as [52]

$$R_{\text{eff}} = (n - 1)f. \quad (3.6)$$

The resonant nuclear contribution to the refractive index of a material can be written as [53],

$$n(E_\gamma) - 1 = \frac{n_{\text{nuc}} \sigma_{\text{res}}(E_\gamma) f_{\text{LM}}}{2E_\gamma} \simeq \frac{2n_{\text{nuc}}}{E_\gamma^3}, \quad (3.7)$$

where, $n_{\text{nuc}} \simeq (\text{keV})^3$ is the nuclei number density in a material, and f_{LM} is the Lamb-Mössbauer factor which is replaced by its resonant value of $2/\pi$ to obtain the last equality. Thus, we obtain the range over which the emitted photons would remain parallel as

$$z_R \simeq \frac{\pi R_{\text{eff}}^2}{\lambda} \sim 3.2 \text{ km} \left(\frac{20 \text{ keV}}{E_\gamma} \right)^5 \left(\frac{f}{1 \text{ m}} \right)^2. \quad (3.8)$$

Thus the flux at the Mössbauer receiver would be the same as the Mössbauer emitter. Using Eq. (3.2) and Eq. (3.3), we obtain

$$\Delta E = \sqrt{\frac{\Gamma(\Delta E)_{\text{SR}}}{(N_\gamma)_{\text{SR}}}} \equiv \sqrt{\frac{\Gamma}{\Phi_{\text{SR}}}}, \quad (3.9)$$

where the spectral flux of a synchrotron source Φ_{SR} is defined as the ratio of the flux per bandwidth. For a given integration time, using the above equation we obtain the sensitivity of the experiment by $\Phi_{\text{SR}} \rightarrow \Phi_{\text{SR}} \times (t_{\text{int}}/\text{s}) \text{ Min} [1, (\tau_{\text{coh}}/t_{\text{int}})^{1/2}]$ [54].

Due to the spread in the energy domain, the emitted photons will have a longitudinal coherence length

of $\sim 2\pi/\Gamma$. Although the relative phase information is regained at twice the distance, we consider a conservative approach, and limit the maximum achievable baseline for a given Mössbauer transition as

$$L \lesssim 200 \text{ m} \left(\frac{\tau_{\text{dec}}}{100 \text{ ns}} \right). \quad (3.10)$$

Furthermore, we require the DM field to remain coherent over the baseline. For a separation of L between the Mössbauer emitter and the absorber, this provides a constraint on DM mass as,

$$m_\phi \lesssim 4.1 \times 10^{-4} \text{ eV} \left(\frac{3 \text{ km}}{L} \right). \quad (3.11)$$

Moreover, to observe a homogeneous shift in the energy levels due to oscillating DM, we require the decay time of the nucleus τ_{dec} , to be shorter than the DM oscillation time. Thus we get,

$$t_{\text{osc}} = \frac{2\pi}{m_\phi} \gtrsim \tau_{\text{dec}} \Rightarrow m_\phi \lesssim 2\pi \tau_{\text{dec}}. \quad (3.12)$$

For DM oscillation frequencies higher than the above limit results in inhomogeneous energy shifts, and produces sidebands around the transition. Combining Eq. (3.11) and Eq. (3.12), we get an upper bound on the DM mass as,

$$m_\phi \lesssim 8.3 \times 10^{-5} \text{ eV} \times \text{Min} \left[\frac{15 \text{ km}}{L}, \frac{50 \text{ ps}}{\tau_{\text{dec}}} \right]. \quad (3.13)$$

IV. MONOCHROMATORS AND BEAMS

Currently several monochromators exist all around the world; such as Advance Photon Lab (APS) in USA [55], ESRF in Europe [56], and SPring-8 in Japan [57]. These are operating in the energy range of $\mathcal{O}(5 - 130)$ keV [49, 58, 59]. To perform SMS of a transition, we require a beamline whose energy range covers the transition energy of the said sample. For example BLXU09 beam line at SPring-8, and 3-ID beam line at the APS are currently being used to perform SMS of various transitions in the range of $(5 - 20)$ keV, whereas the ID18 beam line at ESRF, is being used to perform SMS of various transitions spanning energy range of $(5 - 70)$ keV. To perform SMS with a transition whose energy is higher than 70 keV, 11-ID beam line at the APS can be used. See [46, 47, 49, 59] and refs. therein for a comprehensive list of the elements (along with all the relevant parameters involving each transitions) that can be used to perform SMS.

In Table I, the energy of the first two listed transitions is in the range of $\sim (5 - 20)$ keV. Currently, SMS with ^{181}Ta and ^{57}Fe can be performed with the BLXU09 beam-line (among many others). Currently, this beam line has achieved a flux of $6.3 \times 10^{12} \gamma/\text{s}$ with a bandwidth of 35.7 meV [60]. The transition energy of ^{187}Os is 74.4 keV, and thus can not be probed by the BLXU09 beam [61]. 20-ID-D beam line at the APS [55] is operating in the energy range of 35 – 120 keV, with an obtained flux of $10^{14} \gamma/\text{s}$ at a resolution of 70 eV. This beam line can be used to conduct SMS with ^{187}Os .

V. DETECTION SENSITIVITY

In this section, we consider different interactions of DM with the low energy SM, and calculate the nuclear energy shift due to that interaction.

Let us consider a linear coupling between the ULDM, ϕ , with the up (u), and down (d) quarks, gluons ($G_{\mu\nu}^a$), and photons ($F_{\mu\nu}$) as,

$$\mathcal{L} \supset \sum_{\psi=u,d} -\frac{\phi}{f_\psi} m_\psi \bar{\psi} \psi - \frac{\alpha \phi}{4 f_\gamma} F^2 - \frac{\beta(\alpha_s) \phi}{4\alpha_s f_g} G^2, \quad (5.1)$$

where, $G^2 = G_{a\mu\nu} G^{a\mu\nu}$ with a being the color index, $F^2 = F_{\mu\nu} F^{\mu\nu}$, m_ψ is the mass of ψ , α is the fine structure constant, $\beta(\alpha_s)$ is the beta function of the strong coupling constant α_s , and f_i denotes the interaction strength with various modules.

A. alpha modulus

The coupling $\frac{\alpha \phi}{4 f_\gamma} F^2$ induces an oscillating component to the fine structure constant due to the time dependent ϕ background as given in Eq. (2.1). The shift in α can be written as

$$\alpha \rightarrow \alpha - \frac{\alpha^2 \phi}{f_\gamma} \Rightarrow \frac{\Delta \alpha}{\alpha(0)} = \frac{\alpha(\phi) - \alpha(0)}{\alpha(0)} \simeq -\frac{\alpha \phi}{f_\gamma}. \quad (5.2)$$

The dominant electromagnetic effect in the nuclear energy is encoded in the α dependence of the nucleon masses and nuclear binding energy [67]. Most importantly, due to the change in α , the electromagnetic self energy of a nucleus of size r_{nuc} , with Z protons and A nucleons changes as $\sim Z^2 \Delta \alpha / r_{\text{nuc}}$. As the Mössbauer transitions involve transitions between nearly degenerate energy levels, we estimate

the energy due to one nucleon transition. Thus we obtain the energy shift due to change of α as [42],

$$\Delta E \simeq \frac{Z \Delta \alpha}{r_{\text{nuc}}} \simeq -\frac{Z \alpha^2}{A^{1/3} r_0} \frac{\Delta \phi}{f_\gamma}, \quad (5.3)$$

where, we take the position of the transitioning nucleon to be the nuclear size with $r_{\text{nuc}} = A^{1/3} r_0$, and $r_0 \sim 1.2$ fm is some typical nuclear scale [68].

B. Yukawa modulus

The low energy dynamics of nuclear physics, can largely be described by the physics in the Isospin limit. Thus, we consider ϕ coupling to the Isospin symmetric combination of the u , and d quarks masses. We define $\hat{m} = (m_u + m_d)/2$, and $2\hat{m}/f_{\hat{m}} = (m_u/f_u + m_d/f_d)$, and obtain

$$\hat{m} \rightarrow \hat{m} - \frac{\hat{m} \phi}{f_{\hat{m}}} \Rightarrow \frac{\Delta \hat{m}}{\hat{m}} = \frac{\phi}{f_{\hat{m}}}, \quad (5.4)$$

using Eq. (5.1). As the light quark masses largely affect the pion mass (m_π) as $m_\pi^2 \propto \hat{m}$, we consider the one-pion exchange (OPE) potential between two nucleons to estimate the change in nuclear energy ΔE . Following the notation of [69–71], the OPE potential can be written as,

$$V_{\text{OPE}}(r) = -\frac{g_{\pi NN}^2}{4\pi} \frac{m_\pi^2}{4m_N^2} \frac{e^{-m_\pi r}}{r}, \quad (5.5)$$

where, $g_{\pi NN}^2/(4\pi) = 15$ is the effective pion nucleon interaction strength. For a distance $r \lesssim 1/m_\pi$, we get,

$$\begin{aligned} \Delta E &\simeq \frac{g_{\pi NN}^2}{(4\pi) 4r} \left[\frac{\partial(m_\pi^2/m_N^2)}{\partial \ln m_\pi^2} \frac{\partial \ln m_\pi^2}{\partial \ln \hat{m}} \right] \frac{\Delta \hat{m}}{\hat{m}} \\ &\simeq 12.3 \text{ MeV} \frac{\Delta \phi}{f_{\hat{m}}}, \end{aligned} \quad (5.6)$$

where, we use $\partial \ln m_\pi^2 / \partial \ln \hat{m} = 1$, $\partial \ln m_N / \partial \ln m_\pi^2 \simeq 0.06$ [19], and set $r = r_0$.

C. Gluon modulus

Similar to the α coupling, $\frac{\beta(\alpha_s) \phi}{4\alpha_s f_g} G^2$ interaction shifts the strong coupling constant, and ϕ induced change to α_s can be written as

$$\frac{\Delta \alpha_s}{\alpha_s(0)} = \frac{\alpha_s(\phi) - \alpha_s(0)}{\alpha_s(0)} \simeq -\frac{\beta(\alpha_s) \phi}{\alpha_s f_g}. \quad (5.7)$$

Transition List				Beam		
Transition	E_0 (keV)	Γ_{exp} (eV)	τ_{dec}	$(\Delta E)_{\text{SR}}$	$(N_\gamma)_{\text{SR}}$ γ/s	Φ_{SR} $\gamma/(\text{s} \cdot \text{eV})$
$^{181}_{73}\text{Ta}$ [62]	6.2	5.5×10^{-10}	8.7 μs	35.7 meV	6.3×10^{12}	1.76×10^{14}
$^{57}_{26}\text{Fe}$ [63]	14.4	5×10^{-9}	141.8 ns	35.7 meV	6.3×10^{12}	1.76×10^{14}
$^{187}_{76}\text{Os}$ [64, 65]	74.4	1.2×10^{-5}	0.0534 ns	70 eV	1×10^{14}	1.43×10^{12}

TABLE I: List of relevant parameters for a few Mössbauer transitions that can be used to probe DM (see [46, 47, 49, 59] and refs. therein for a more comprehensive list of the elements along with all the relevant synchrotron source parameters involving each transitions, that can be used to perform SMS). The listed transitions are chosen as benchmarks and also to highlight various facets of our proposed method. We divide the table in two main columns: “Transition List” - providing information about a specific transition, and “Beam” - providing information about currently operating synchrotron beam that can be used to perform a SMS of that specific transition. Left to right: we outline a transition, its energy E_0 , experimentally observed line width, Γ_{exp} , decay time τ_{dec} , the energy resolution $(\Delta E)_{\text{SR}}$, the flux $(N_\gamma)_{\text{SR}}$ per second, and the spectral flux $\Phi_{\text{SR}} = (N_\gamma)_{\text{SR}}/(\Delta E)_{\text{SR}}$ of the synchrotron source. We quote the experimentally observed line-widths for ^{181}Ta , and ^{57}Fe , whereas for ^{187}Os we obtain it from the observed decay time. Note that, for ^{181}Ta , the observed line width is broadened compare to the natural one by almost a factor of 7.5 [66]. In such case, one should use the observed width to estimate the sensitivity.

As the QCD scale Λ_{QCD} , depends on α_s , we obtain the ϕ dependence of Λ_{QCD} as,

$$\frac{\partial \ln \Lambda_{\text{IR}}}{\partial \phi} \simeq -\frac{\alpha_s}{\beta(\alpha_s)} \frac{\partial \ln \alpha_s}{\partial \phi} = \frac{1}{f_g}, \quad (5.8)$$

using Eq. (5.7). To calculate the change in the nuclear energy due to the ϕ dependence of α_s , we note that any shift in Λ_{QCD} corresponds to a change in the whole hadronic spectrum. A small ϕ induced change can be estimated by considering OPE potential with ϕ dependent pion-nucleon coupling constant as,

$$\begin{aligned} \Delta E &\simeq \left[\frac{g_{\pi NN}^2/(4\pi)}{4r_0} \frac{\partial(m_\pi^2/m_N^2)}{\partial \ln \Lambda_{\text{IR}}} \frac{\Delta \Lambda_{\text{IR}}}{\Lambda_{\text{IR}}} \right. \\ &\quad \left. + \frac{m_\pi^2}{4r_0 m_N^2} \frac{\partial(g_{\pi NN}^2/4\pi)}{\partial \ln \alpha_s} \frac{\Delta \alpha_s}{\alpha_s} \right] \\ &\simeq 0.1 \text{ GeV} \frac{\Delta \phi}{f_g}, \end{aligned} \quad (5.9)$$

where we use $\partial \ln(g_{\pi NN}^2/4\pi)/\partial \ln \alpha_s = 1$.

VI. RESULTS AND DISCUSSION

To illustrate the reach of our proposed method, we list a few transitions with decay time ranging from $\tau_{\text{dec}} \sim \mathcal{O}(10 \mu\text{s})$ to $\mathcal{O}(50 \text{ ps})$ and transition energy from $E_0 \sim (5 - 75) \text{ keV}$ in Table I. Using the listed transitions as benchmarks, we show the parameter space of various dark matter-SM interaction in Fig. 2 and Fig. 3. We plot the parameter space for each module by equating the DM induced the

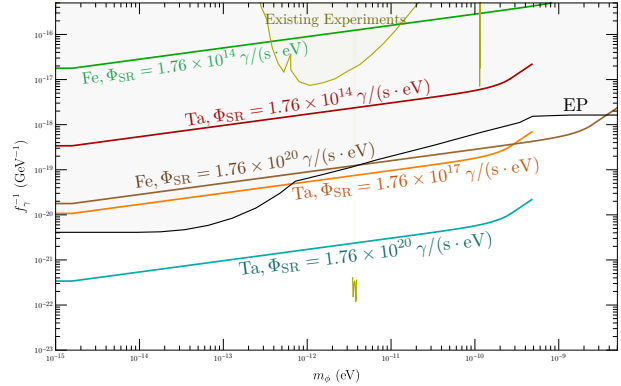


FIG. 2: Parameter space of the DM-photon interaction strength f_γ^{-1} , as a function of DM mass m_ϕ . The reach of the proposed experiment with existing synchrotron spectral flux are shown by the red (^{181}Ta) and green (^{57}Fe) lines. See Table I for more details. Reach of a Mössbauer experiment with improved spectral flux with different nuclei are also depicted: orange (10^3 with ^{181}Ta), turquoise (10^6 with ^{181}Ta), and brown (10^6 with ^{57}Fe). The projections are shown for the integration time of 1 month, and the maximal achievable baseline.

The gray and the yellow shaded regions depict the bound from various equivalence principle (EP) violating tests [72–74] and existing DM search experiments [26, 75, 76] respectively.

energy shifts, i.e Eqs. (5.6, 5.3, 5.9) with Eq. (3.9) for an integration time of 1 month. Choosing a variety of Mössbauer nuclei with different decay times enables us to probe ULDM over a wide range of frequencies. As can be seen from Eq. (3.13), a

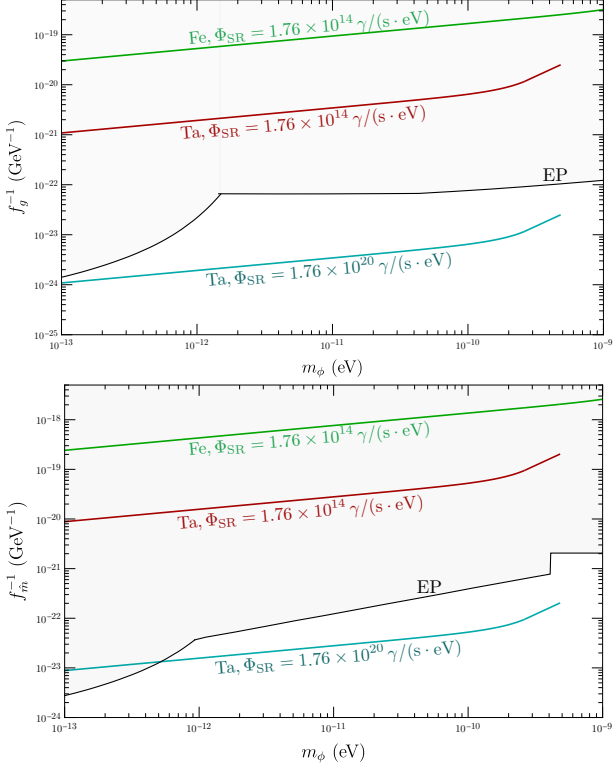


FIG. 3: Parameter space of the DM-gluon f_g^{-1} (top), and DM-quarks f_m^{-1} (bottom) interaction strength as a function of DM mass m_ϕ . Existing experimental bounds are taken from [77]. Remaining description matches the caption of Fig. 2.

Mössbauer spectroscopy with ^{187}Os would allow us to probe ULDM mass upto ~ 10 GHz, whereas with ^{181}Ta and ^{57}Fe nuclei, the reach is limited upto ~ 1 MHz. On the other hand, maximum achievable baseline with ^{181}Ta is ~ 2 km as opposed to a 10 cm for ^{187}Os as can be seen from Eq. (3.10) [78]. On top of this, the sensitivity of the experiment scales as $\Delta E \propto 1/\tau_{\text{dec}}^{1/2}$ (c.f. Eq. (3.9)). Thus, overall with current technology, a Mössbauer nuclei with larger decay time is better suited for probing DM.

In Fig. 2 and Fig. 3, the reach of a synchrotron based Mössbauer experiment with ^{181}Ta and ^{57}Fe nuclei with currently available spectral flux of $\Phi_{\text{SR}} = 1.76 \times 10^{14} \gamma/(\text{s} \cdot \text{eV})$ are shown by the red and the green lines respectively. The orange, turquoise and brown lines depict the reach a Mössbauer experiment with improved synchrotron beam lines. The first two projections are made with ^{181}Ta with an improved spectral flux of 10^3 and 10^6 respectively, whereas for the brown lines, we consider ^{57}Fe with 10^6 improvement. All the projections

are shown with the maximum achievable baseline for the given transition. Constraints from the existing ULD M searches are shown in yellow shaded region [26], whereas the solid black lines represent the bound from various equivalence principle (EP) violation searches [72–74, 79].

To understand the projections, in the low mass regime, i.e. for $m_\phi \lesssim 1/L$, the sensitivity of the experiment remains independent of DM mass for a phase coherent signal. Dictated by the integration time, we obtain maximum experimental sensitivity for $m_\phi \lesssim 2\pi/(t_{\text{int}}\beta^2) \simeq 2 \times 10^{-15}$ eV. Beyond the coherence time, the sensitivity decreases as $m_\phi^{1/4}$ till $m_\phi \sim 1/L$, and in the high mass regime, it scales as $m_\phi^{5/4}$. These scaling behaviours can be seen from Fig. 2 and Fig. 3.

The reach of the proposed experiment with existing synchrotron beam lines is at par with the bounds coming from the EP violation searches. For the scalar-photon interaction strength the obtained reach is within a factor of $\mathcal{O}(10)$ of the EP limits, whereas for f_g and f_m , the obtained bounds are weaker by $\mathcal{O}(10^2)$. As the experimental sensitivity is $\propto \Phi_{\text{SR}}^{1/2}$, an improvement of $\mathcal{O}(10^2)$ ($\mathcal{O}(10^4)$) in spectral flux would enable us to probe hitherto uncharted territory for f_γ (f_g and f_m). Nonetheless, even with existing set up, a SMS with ^{181}Ta would provide the best bound on DM-SM interaction strength; by improving the existing limits coming exclusively from experiments searching for time oscillating signals by several orders of magnitude.

A large number of beam lines are currently operating with bandwidth as low as 10^{-8} eV [80], and a flux as high as $4 \times 10^{13} \gamma/\text{s}$ [55, 57]. As the experimental reach depends on the spectral flux, an improvement in either the synchrotron bandwidth or the flux (or both) will vastly extend the reach of DM detection. Several beam lines are already working on implementing changes to obtain higher spectral flux while maintaining a good energy resolution. For example, the 3-ID beam line at the APS is already operating in several modes achieving spectral flux in the range of $(5 \times 10^{11} - 2 \times 10^{13}) \gamma/(\text{s} \cdot \text{eV})$ ($N_\gamma = 5 \times 10^9 \gamma/\text{s}$ with a resolution of 10 meV, and/or flux of $2 \times 10^{13} \gamma/\text{s}$ with $(\Delta E)_{\text{SR}} \sim \text{eV}$) [55]. Their aim is to reach a resolution of 0.6 meV while maintaining a high flux [58]. This would lead to a spectral flux of $\Phi_{\text{SR}} \simeq 3 \times 10^{17} \gamma/(\text{s} \cdot \text{eV})$, resulting

in an immediate improvement of $\mathcal{O}(10^3)$ over the existing setup.

With an improved spectral flux of $\mathcal{O}(10^3)$, a ^{181}Ta based Mössbauer experiment would enable us to probe DM-photon interaction in the 100 Hz - 100 kHz frequency range beyond the EP limits. It would extend the DM search by a factor of $\mathcal{O}(10)$ in the coupling strength as shown by the orange line in Fig. 2. As a target for the synchrotron facilities, in Fig. 2 and 3, we show the experimental reach with an improved spectral flux of $\mathcal{O}(10^6)$ by the turquoise and the green lines for ^{181}Ta and ^{57}Fe respectively. This would further enable us to explore the DM parameter space upto MHz frequency with DM-photon coupling strength as low as $f_\gamma \sim 3 \times 10^{22} \text{ GeV}$. Thus the reach of DM search would be extended by more than two orders of magnitude beyond the current limits. For DM-gluon coupling, a Mössbauer experiment with ^{181}Ta would be able to probe previously unexcluded part of the parameter space in the mass range of $10^{-21} \text{ eV} \lesssim m_\phi \lesssim 5 \times 10^{-10} \text{ eV}$. It would extend the DM search upon improving the existing EP limits on f_g^{-1} by two orders of magnitude. For the Yukawa coupling, the improvement over EP limits is limited to $5 \times 10^{-13} \text{ eV} \lesssim m_\phi \lesssim 5 \times 10^{-10} \text{ eV}$ and a factor of 5 on $f_{\hat{m}}$. As previously discussed, an improved Mössbauer experiment would yield the best bound on DM-photon coupling in the kHz-MHz frequency range, even when compared to other proposed experiments [26]. For the DM coupling with the quarks and gluons, no currently proposed experiments can surpass the EP limits for frequencies above 100 Hz, despite the recent insight from the 8.3 eV transition of ^{229}Th [81]. This highlights the complementarity of the proposed experiment to conventional probes.

CONCLUSION

Motivated by the lack of current and future experimental efforts, in this work, we propose the possibility of probing ultra-light scalar dark matter (DM) by synchrotron radiation based Mössbauer spectroscopy in the kHz-MHz mass range. Despite their exquisite sensitivity, any frequency comparison tests of ultra-light scalar DM, has extremely limited reach in the high frequency region. Thus our proposed experiment is complementary to the conventional probes.

We have analysed the reach of the proposed

method in probing DM interaction with various standard model (SM) fields. We have shown that with existing synchrotron beams, the reach of a Mössbauer experiment is at par with the most stringent limits from various equivalence principle (EP) violation searches. An improvement of the set up would enable us to probe hitherto uncharted territory of the dark matter parameter space; by extending the DM search by several orders of magnitude beyond the EP limits.

Mössbauer spectroscopy is a well-established technique that plays a crucial role in the fields of chemistry and biology. With the advent of powerful synchrotron sources, synchrotron radiation-based Mössbauer spectroscopy has become increasingly significant. Moreover, existing synchrotron sources are continuously improving their facilities, regardless of their application in fundamental physics. In this work, we demonstrate that Mössbauer spectroscopy can serve as an excellent sensor for dark matter, especially by extending the DM search to the high-frequency region. Thus, this technique complements conventional atomic and nuclear setups. Furthermore, this work could be used as a physics target to enhance synchrotron facilities which in turn would further extend its sensitivity as a DM sensor.

ACKNOWLEDGEMENT

The author would like to thank Surjeet Rajendran for collaboration in the early phase of the project. His critical comments and discussions were extremely useful in shaping the work. The author also thanks Ercan Alp for useful comments regarding the longitudinal coherence length. The author also thanks Roni Harnik, Anson Hook, Shmuel Nussinov, Gilad Perez, and Marianna Safronova for their useful comments. The work of AB is supported by NSF grant PHY-2210361 and the Maryland Center for Fundamental Physics.

-
- [1] E. W. Kolb and M. S. Turner, *The Early Universe*, Vol. 69 (1990).
- [2] R. D. Peccei and H. R. Quinn, Constraints Imposed by CP Conservation in the Presence of Instantons, *Phys. Rev. D* **16**, 1791 (1977).
- [3] R. D. Peccei and H. R. Quinn, CP Conservation in the Presence of Instantons, *Phys. Rev. Lett.* **38**, 1440 (1977).
- [4] F. Wilczek, Problem of Strong P and T Invariance in the Presence of Instantons, *Phys. Rev. Lett.* **40**, 279 (1978).
- [5] J. E. Kim, Weak Interaction Singlet and Strong CP Invariance, *Phys. Rev. Lett.* **43**, 103 (1979).
- [6] M. A. Shifman, A. I. Vainshtein, and V. I. Zakharov, Can Confinement Ensure Natural CP Invariance of Strong Interactions?, *Nucl. Phys. B* **166**, 493 (1980).
- [7] A. R. Zhitnitsky, On Possible Suppression of the Axion Hadron Interactions. (In Russian), *Sov. J. Nucl. Phys.* **31**, 260 (1980).
- [8] S. Weinberg, A New Light Boson?, *Phys. Rev. Lett.* **40**, 223 (1978).
- [9] M. Dine, W. Fischler, and M. Srednicki, A Simple Solution to the Strong CP Problem with a Harmless Axion, *Phys. Lett. B* **104**, 199 (1981).
- [10] M. Dine and W. Fischler, The Not So Harmless Axion, *Phys. Lett. B* **120**, 137 (1983).
- [11] E. G. Adelberger, B. R. Heckel, and A. E. Nelson, Tests of the gravitational inverse square law, *Ann. Rev. Nucl. Part. Sci.* **53**, 77 (2003), [arXiv:hep-ph/0307284](#).
- [12] P. W. Graham, D. E. Kaplan, and S. Rajendran, Cosmological Relaxation of the Electroweak Scale, *Phys. Rev. Lett.* **115**, 221801 (2015), [arXiv:1504.07551 \[hep-ph\]](#).
- [13] T. Flacke, C. Frugiuele, E. Fuchs, R. S. Gupta, and G. Perez, Phenomenology of relaxion-Higgs mixing, *JHEP* **06**, 050, [arXiv:1610.02025 \[hep-ph\]](#).
- [14] A. Banerjee, H. Kim, O. Matsedonskyi, G. Perez, and M. S. Safronova, Probing the Relaxed Relaxion at the Luminosity and Precision Frontiers, *JHEP* **07**, 153, [arXiv:2004.02899 \[hep-ph\]](#).
- [15] A. Hook, Solving the Hierarchy Problem Discretely, *Phys. Rev. Lett.* **120**, 261802 (2018), [arXiv:1802.10093 \[hep-ph\]](#).
- [16] L. F. Abbott and P. Sikivie, A Cosmological Bound on the Invisible Axion, *Phys. Lett. B* **120**, 133 (1983).
- [17] J. Preskill, M. B. Wise, and F. Wilczek, Cosmology of the Invisible Axion, *Phys. Lett. B* **120**, 127 (1983).
- [18] A. Banerjee, H. Kim, and G. Perez, Coherent relaxion dark matter, *Phys. Rev. D* **100**, 115026 (2019), [arXiv:1810.01889 \[hep-ph\]](#).
- [19] H. Kim and G. Perez, Oscillations of atomic energy levels induced by QCD axion dark matter, *Phys. Rev. D* **109**, 015005 (2024), [arXiv:2205.12988 \[hep-ph\]](#).
- [20] K. Blum, R. T. D’Agnolo, M. Lisanti, and B. R. Safdi, Constraining Axion Dark Matter with Big Bang Nucleosynthesis, *Phys. Lett. B* **737**, 30 (2014), [arXiv:1401.6460 \[hep-ph\]](#).
- [21] A. Banerjee, G. Perez, M. Safronova, I. Savoray, and A. Shalit, The phenomenology of quadratically coupled ultra light dark matter, *JHEP* **10**, 042, [arXiv:2211.05174 \[hep-ph\]](#).
- [22] D. Brzeminski, Z. Chacko, A. Dev, and A. Hook, Time-varying fine structure constant from naturally ultralight dark matter, *Phys. Rev. D* **104**, 075019 (2021), [arXiv:2012.02787 \[hep-ph\]](#).
- [23] M. S. Safronova, D. Budker, D. DeMille, D. F. J. Kimball, A. Derevianko, and C. W. Clark, Search for new physics with atoms and molecules, *Rev. Mod. Phys.* **90**, 025008 (2018).
- [24] D. Antypas, D. Budker, V. V. Flambaum, M. G. Kozlov, G. Perez, and J. Ye, Fast apparent oscillations of fundamental constants, *Annalen Phys.* **532**, 1900566 (2020), [arXiv:1912.01335 \[physics.atom-ph\]](#).
- [25] A. Arvanitaki, J. Huang, and K. Van Tilburg, Searching for dilaton dark matter with atomic clocks, *Phys. Rev. D* **91**, 015015 (2015), [arXiv:1405.2925 \[hep-ph\]](#).
- [26] D. Antypas *et al.*, New Horizons: Scalar and Vector Ultralight Dark Matter, in *2022 Snowmass Summer Study* (2022) [arXiv:2203.14915 \[hep-ex\]](#).
- [27] M. Filzinger, S. Dörscher, R. Lange, J. Klose, M. Steinel, E. Benkler, E. Peik, C. Lisdat, and N. Huntemann, Improved Limits on the Coupling of Ultralight Bosonic Dark Matter to Photons from Optical Atomic Clock Comparisons, *Phys. Rev. Lett.* **130**, 253001 (2023), [arXiv:2301.03433 \[physics.atom-ph\]](#).
- [28] A. Banerjee, D. Budker, M. Filzinger, N. Huntemann, G. Paz, G. Perez, S. Porsev, and M. Safronova, Oscillating nuclear charge radii as sensors for ultralight dark matter (2023) [arXiv:2301.10784 \[hep-ph\]](#).
- [29] C. J. Kennedy, E. Oelker, J. M. Robinson, T. Bothwell, D. Kedar, W. R. Milner, G. E. Marti, A. Derevianko, and J. Ye, Precision metrology meets cosmology: Improved constraints on ultralight dark matter from atom-cavity frequency comparisons, *Phys. Rev. Lett.* **125**, 201302 (2020).
- [30] T. Kobayashi, A. Takamizawa, D. Akamatsu, A. Kawasaki, A. Nishiyama, K. Hosaka, Y. Hisai, M. Wada, H. Inaba, T. Tanabe, and M. Yasuda, Search for ultralight dark matter from long-term frequency comparisons of optical and microwave atomic clocks, *Phys. Rev. Lett.* **129**, 241301 (2022).

- [31] R. L. Mössbauer, Kernresonanzfluoreszenz von gammastrahlung in ir 191, *Zeitschrift für Physik* **151**, 124 (1958).
- [32] R. L. Mössbauer, Kernresonanzabsorption von γ -strahlung in ir191, *Zeitschrift für Naturforschung A* **14**, 211 (1959).
- [33] R. Mössbauer, The discovery of the mössbauer effect., *Hyperfine Interactions* **126** (2000).
- [34] P. Gütlich, C. Schröder, and V. Schünemann, Mössbauer spectroscopy—an indispensable tool in solid state research, *Spectroscopy Europe* **24**, 21 (2012).
- [35] S. Nasu, General introduction to mössbauer spectroscopy, in *Mössbauer Spectroscopy: Tutorial Book* (Springer, 2012) pp. 1–22.
- [36] N. N. Greenwood, *Mössbauer spectroscopy* (Springer Science & Business Media, 2012).
- [37] Note that the sensitivity of the proposed setup to vector interactions is typically suppressed, unlike the case for scalar and tensor interactions.
- [38] D. Budker, P. W. Graham, M. Ledbetter, S. Rajendran, and A. Sushkov, Proposal for a Cosmic Axion Spin Precession Experiment (CASPER), *Phys. Rev. X* **4**, 021030 (2014), [arXiv:1306.6089 \[hep-ph\]](https://arxiv.org/abs/1306.6089).
- [39] A. Derevianko, Detecting dark-matter waves with a network of precision-measurement tools, *Phys. Rev. A* **97**, 042506 (2018), [arXiv:1605.09717 \[physics.atom-ph\]](https://arxiv.org/abs/1605.09717).
- [40] O. Svelto, *Principles of Lasers*, 5th ed. (Springer New York, NY, 2010) pp. XXI, 620.
- [41] We have omitted the factors involving the spins of the transition states, and the internal conversion factors [43].
- [42] G. Gratta, D. E. Kaplan, and S. Rajendran, Searching for New Interactions at Sub-micron Scale Using the Mossbauer Effect, *Phys. Rev. D* **102**, 115031 (2020), [arXiv:2010.03588 \[hep-ph\]](https://arxiv.org/abs/2010.03588).
- [43] W. Sturhahn, Nuclear resonant spectroscopy, *Journal of Physics: Condensed Matter* **16**, S497 (2004).
- [44] J. B. Hastings, D. P. Siddons, U. van Bürck, R. Holatz, and U. Bergmann, Mössbauer spectroscopy using synchrotron radiation, *Phys. Rev. Lett.* **66**, 770 (1991).
- [45] E. Gerdau, R. Rüffer, H. Winkler, W. Tolksdorf, C. P. Klages, and J. P. Hannon, Nuclear bragg diffraction of synchrotron radiation in yttrium iron garnet, *Phys. Rev. Lett.* **54**, 835 (1985).
- [46] O. Leupold, Hyperfine spectroscopy with nuclear resonant scattering of synchrotron radiation, in *Mössbauer Spectroscopy*, edited by P. Gütlich, B. W. Fitzsimmons, R. Rüffer, and H. Spiering (Springer Netherlands, Dordrecht, 2003) pp. 21–32.
- [47] M. Seto, R. Masuda, Y. Kobayashi, S. Kitao, M. Kurokuzu, M. Saito, S. Hosokawa, H. Ishibashi, T. Mitsui, Y. Yoda, and K. Mibu, Evolution of synchrotron-radiation-based mössbauer absorption spectroscopy for various isotopes, *Hyperfine Interactions* **238**, 78 (2017).
- [48] A. I. Chumakov and W. Sturhahn, Experimental aspects of inelastic nuclear resonance scattering, *Hyperfine Interactions* **123**, 781 (1999).
- [49] Y. Yoda, X-ray beam properties available at the nuclear resonant scattering beamline at SPring-8, *Hyperfine Interactions* **240**, 72 (2019).
- [50] G. V. Smirnov, General properties of nuclear resonant scattering, *Hyperfine Interactions* **123**, 31 (1999).
- [51] A. I. Chumakov, A. Q. R. Baron, I. Sergueev, C. Strohm, O. Leupold, Y. Shvyd'ko, G. V. Smirnov, R. Rüffer, Y. Inubushi, M. Yabashi, K. Tono, T. Kudo, and T. Ishikawa, Superradiance of an ensemble of nuclei excited by a free electron laser, *Nature Physics* **14**, 261 (2018).
- [52] E. Hecht, *Optics* (Fourth edition. Reading, Mass. : Addison-Wesley, [2002] ©2002).
- [53] M. Blume and O. C. Kistner, Resonant absorption in the presence of faraday rotation, *Phys. Rev.* **171**, 417 (1968).
- [54] Note that, in Tab. I, $(N_\gamma)_{\text{SR}} (\Phi_{\text{SR}})$ is given in the unit of γ/s ($\gamma/\text{eV} \cdot \text{s}$) where here it is dimensionless (γ/eV).
- [55] <https://www.aps.anl.gov/Beamlines/Directory>.
- [56] <https://www.esrf.fr/home/UsersAndScience/find-a-beamline.html>.
- [57] http://www.spring8.or.jp/en/about_us/whats_sp8/facilities/bl/list/.
- [58] T. E. Fornek, Advanced photon source upgrade project final design report [10.2172/1543138](https://arxiv.org/abs/10.2172/1543138) (2019).
- [59] Y. Yoda, X. Zhang, and S. Kikuta, High-Resolution Monochromators for Nuclear Resonant Scattering Developed at BL09XU, SPring-8, *AIP Conference Proceedings* **879**, 926 (2007), https://pubs.aip.org/aip/acp/article-pdf/879/1/926/11680254/926_1_online.pdf.
- [60] A. Yasui, Y. Takagi, T. Osaka, Y. Senba, H. Yamazaki, T. Koyama, H. Yumoto, H. Ohashi, K. Motomura, K. Nakajima, *et al.*, B109xu: an advanced hard x-ray photoelectron spectroscopy beamline of spring-8, *Journal of Synchrotron Radiation* **30** (2023).
- [61] ^{187}Os has another transition with decay time of 3.4 ns and $E_0 \sim 10 \text{ keV}$ [65, 82]. BLXU09/3-ID beam can be used to conduct SMS of this isotope.
- [62] S. C. Wu, Nuclear Data Sheets for $A = 181$, *Nucl. Data Sheets* **106**, 367 (2005).
- [63] M. R. Bhat, Nuclear Data Sheets for $A = 57$, *Nucl. Data Sheets* **85**, 415 (1998).
- [64] S. G. Malmkog, V. Berg, B. Fogelberg, and A. Bäcklin, On the low-energy band structure in ^{187}Os , *Nucl. Phys. A* **166**, 573 (1971).
- [65] M. S. Basunia, Nuclear Data Sheets for $A = 187$, *Nucl. Data Sheets* **110**, 999 (2009).

- [66] V. Dornow, J. Binder, A. Heidemann, G. Kalvius, and G. Wortmann, Preparation of narrow-line sources for the 6.2 keV mössbauer resonance of ^{181}Ta , *Nuclear Instruments and Methods* **163**, 491 (1979).
- [67] T. Damour and J. F. Donoghue, Equivalence Principle Violations and Couplings of a Light Dilaton, *Phys. Rev. D* **82**, 084033 (2010), [arXiv:1007.2792 \[gr-qc\]](#).
- [68] K. Krane, *Introductory Nuclear Physics* (Wiley, 1991).
- [69] R. Machleidt, K. Holinde, and C. Elster, The Bonn Meson Exchange Model for the Nucleon Nucleon Interaction, *Phys. Rept.* **149**, 1 (1987).
- [70] R. Machleidt and I. Slaus, The Nucleon-nucleon interaction: Topical review, *J. Phys. G* **27**, R69 (2001), [arXiv:nucl-th/0101056](#).
- [71] H. Murayama, Lecture notes on many body problems, <http://hitoshi.berkeley.edu/221B-S01/8.pdf>.
- [72] P. Touboul *et al.* (MICROSCOPE), MICROSCOPE Mission: Final Results of the Test of the Equivalence Principle, *Phys. Rev. Lett.* **129**, 121102 (2022).
- [73] S. Schlamminger, K. Y. Choi, T. A. Wagner, J. H. Gundlach, and E. G. Adelberger, Test of the equivalence principle using a rotating torsion balance, *Phys. Rev. Lett.* **100**, 041101 (2008), [arXiv:0712.0607 \[gr-qc\]](#).
- [74] G. L. Smith, C. D. Hoyle, J. H. Gundlach, E. G. Adelberger, B. R. Heckel, and H. E. Swanson, Short range tests of the equivalence principle, *Phys. Rev. D* **61**, 022001 (2000).
- [75] E. Savalle, A. Hees, F. Frank, E. Cantin, P.-E. Pottie, B. M. Roberts, L. Cros, B. T. McAllister, and P. Wolf, Searching for dark matter with an optical cavity and an unequal-delay interferometer, *Phys. Rev. Lett.* **126**, 051301 (2021).
- [76] S. M. Vermeulen *et al.*, Direct limits for scalar field dark matter from a gravitational-wave detector., *Nature* **600**, 424 (2021).
- [77] R. Oswald *et al.*, Search for Dark-Matter-Induced Oscillations of Fundamental Constants Using Molecular Spectroscopy, *Phys. Rev. Lett.* **129**, 031302 (2022), [arXiv:2111.06883 \[hep-ph\]](#).
- [78] Note that, this is a conservative estimate, and tweaking the set-up may result in a baseline not restricted by this requirement.
- [79] T. A. Wagner, S. Schlamminger, J. H. Gundlach, and E. G. Adelberger, Torsion-balance tests of the weak equivalence principle, *Class. Quant. Grav.* **29**, 184002 (2012), [arXiv:1207.2442 \[gr-qc\]](#).
- [80] T. Mitsui, R. Masuda, S. Kitao, Y. Kobayashi, and M. Seto, Rayleigh scattering of synchrotron mössbauer radiation using a variable bandwidth nuclear bragg monochromator, *Journal of the Physical Society of Japan* **91**, 064001 (2022).
- [81] E. Fuchs, F. Kirk, E. Madge, C. Paranjape, E. Peik, G. Perez, W. Ratzinger, and J. Tiedau, Implications of the laser excitation of the Th-229 nucleus for dark matter searches (2024) [arXiv:2407.15924 \[hep-ph\]](#).
- [82] D. Bessas, I. Sergueev, D. G. Merkel, A. I. Chumakov, R. Ruffer, A. Jafari, S. Kishimoto, J. A. Wolny, V. Schünemann, R. J. Needham, P. J. Sadler, and R. P. Hermann, Nuclear resonant scattering of synchrotron radiation by ^{187}Os , *Phys. Rev. B* **91**, 224102 (2015).